

## DYNAMIC BUCKLING OF THIN-WALLED CYLINDRICAL SHELLS UNDER RADIAL IMPACT PRESSURES RANDOMLY DISTRIBUTED IN THE CIRCUMFERENTIAL DIRECTION

YANZE LI, JIAWEI FU

*School of Mechanical Engineering, Nanjing University of Science and Technology, Nanjing, Jiangsu, China*  
*corresponding author J.W. Fu, e-mail: jwfu@njust.edu.cn*

LINFANG QIAN

*School of Mechanical Engineering, Nanjing University of Science and Technology, Nanjing, Jiangsu, China, and*  
*Northwest Institute of Mechanical and Electrical Engineering, Xi'an, Shaanxi, China*

SHIYU CHEN

*School of Mechanical Engineering, Nanjing University of Science and Technology, Nanjing, Jiangsu, China*

Dynamic buckling of thin-walled cylindrical shells under radial impact pressures randomly distributed in the circumferential direction is investigated by extending widely-used Donnell's shell theory. The buckling model proposed here specifically includes nonlinear terms in the geometrical equation and the curvature change due to significant variation of the shell radius. The finite difference method is adopted to solve the equations, and a parameter is defined to describe the buckling degree of the shell. Numerical results show that nonlinear terms from Green's strain tensors and the change of curvature are important for shell large deformation. Pressure characteristics, materials and thickness of the cylindrical shell affect its buckling behavior remarkably.

*Keywords:* cylindrical shell, dynamic buckling, randomly radial impact, nonlinear effects

### 1. Introduction

As a common structure, thin-walled cylindrical shells are extensively used in the field of aerospace, navigation and mining industries (Kumar *et al.*, 2011; Sahu and Datta, 2007; Teng, 1996). In the shell structures, buckling usually becomes a dominated failure pattern rather than damage due to material strength, which is often related to deformation of a structure experiencing a sudden and distinct change when a loading reaches or exceeds a critical value. Buckling analysis of cylindrical shells has been an old but significant topic for a long time and works dealing with this problem are numerous. In static buckling problems, the bearing capacity or critical loading at which the structure buckles is evaluated (Hutchinson, 1965, 2016), however in dynamic buckling problems take the inertia effect as an additive and important factor (Karagiozova and Alves, 2008).

Although dynamic buckling of thin-walled shells under axial loadings has been studied a lot (An *et al.*, 2016; Darabi and Ganesan, 2016; Xu *et al.*, 2006), such a problem of shells under radial pressures received relatively less attention. It should be noted that when thin-walled metallic cylindrical shells are subjected to explosive loadings having significant radial components inward, dynamic buckling becomes an important design consideration. Examples include magnetic confinement devices for producing intense transient magnetic fields (Bykov and Dolotenko, 2015), shape-charge weapons (Saran *et al.*, 2013) or oil well perforators (Farid, 2012) to produce high-velocity metallic jets. Ideally, if the pressure uniformly distributed around the outer surface of a circular cylindrical shell, the shell can move inward without buckling. The

cross section of the shell could remain circular with a decrease of radius over time. However, practically non-axisymmetric motion usually occurs and wrinkles appear on the deformed shells.

The dynamic buckling of thin-walled shells under radial pressures can be caused by defects or disturbances that exist in the manufacturing or application process of the shell (Jones and Okawa, 1976). Geometrically, the initially non-circular shape is frequently regarded as the main factor to make the shell buckle (Ben-Haim, 1993; Elishakoff, 2000; Lindberg, 1992a,b; Wei and Batra, 2006). As to the external loadings, Kumar *et al.* (2015) studied stability of thin-walled cylindrical shells subjected to radial pressures distributed uniformly in the circumferential direction and vibrating over time. In 1987, Lindberg and Florence (1987) systematically studied dynamic pulse buckling behavior of thin-walled cylindrical shells under radial impulses. The impulse effect was equivalently transformed into the initial velocity of the wall with the form of white noise in the circumferential direction. Gu *et al.* (1996) also discussed dynamic plastic buckling of cylindrical shells and rings subjected to initially non-axisymmetric impulsive velocities.

In order to describe deformation behavior of thin-walled cylindrical shells, different models on the premise of various hypotheses have been proposed over the years. Several shell theories, including Donnell's, Novozhilov, Flügge-Lur -Byrne, and Sanders and Koiter have been developed and widely employed (Amabili and Pa doussis, 2003). Amabili (2008) provided a comprehensive overview on these theories. Kumar *et al.* (2015) studied stability of thin-walled cylindrical shells subjected to radial pressures by adopting the Fl gge-Lur -Byrne shell theory. But nonlinear terms in the strain-displacement relations were not included in the above works. Xue *et al.* (2013) extended Donnell's shell theory by considering the effect of large deformation on curvature of the shell, and analyzed the large deformation problem of long shells. Lindberg and Florence (1987) developed the equation of motion without any nonlinear terms according to Donnell's theory to study the dynamic pulse buckling of a cylindrical shell under impulsive loadings. Besides, only the radial displacement was maintained in Lindberg's equations (Lindberg and Florence, 1987). However, linear geometrical equations are limited to infinitesimal deformations, and nonlinear effects due to large deformations are definitely necessary to describe buckling behavior accurately. Another nonlinearity originating from material properties of non-homogeneous materials, such as laminated composite materials and functionally graded materials (Kundalwal and Shingare, 2020; Suresh Kumar *et al.*, 2017), is temporarily out of concern in the current work.

A new buckling model taking nonlinear terms in the geometrical equation and curvature change due to large deformation into account is proposed to investigate the dynamic buckling of a thin-walled cylindrical shell under radial impact pressures randomly distributed in the circumferential direction. The nonlinear partial differential equation (PDE) is solved by the finite difference method (FDM). Subsequently, the effects of pressure characteristics, shell material and thickness on the buckling behavior are discussed.

## 2. Basic equations

As illustrated in Fig. 1, a thin-walled cylindrical shell with radius  $R$  and thickness  $h$  is considered. The middle surface where the origin of the coordinate system is located divides the thickness of the shell equally.  $u_1$ ,  $u_2$  and  $u_3$  are displacements of a generic point of the shell with coordinates  $(x, \theta, z)$  along the axial, circumferential and radial directions, respectively. The displacements of a point in the middle surface along corresponding directions are denoted by  $u$ ,  $v$  and  $w$ . In this paper, the outer surface of the shell is subjected to an impact pressure that is randomly distributed along the circumferential direction. The dynamic buckling is investigated by considering non-linear effects of large deformation within Donnell's theory.

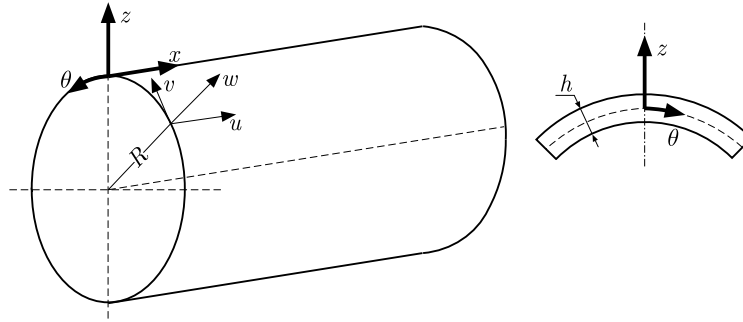


Fig. 1. A thin-walled cylindrical shell

The following assumptions are adopted to study the buckling:

- (H1) The shell is thin, namely,  $h/R \leq 1/10$  (Lindberg and Florence, 1987).
- (H2) The Kirchhoff-Love shell assumption holds, that is stresses in the direction normal to the shell middle surface are negligible, and strains vary linearly along the thickness.
- (H3) The cylindrical shell is infinitely long. Therefore, all the quantities along the axial direction as well as the axial displacement can be regarded as constant.

Based on assumption (H2), the displacements of a generic point in the shell can be expressed in terms of the displacements of a point in the mid-surface which shares the same radial line with the generic point, as

$$u_1 = u(x, \theta) - z\Theta_1 \quad u_2 = v(x, \theta) - z\Theta_2 \quad u_3 = w(x, \theta) \tag{2.1}$$

where the quantities  $\Theta_1$  and  $\Theta_2$  involve the mid-surface displacements and their derivatives, and different shell theories may propose different expressions for them.

For large deformation problems, the geometrical equations in terms of nonlinear Green's strain tensor should be used instead of Cauchy's strain tensor. In cylindrical coordinates, Green's strain components,  $\varepsilon_{xx}$ ,  $\varepsilon_{\theta\theta}$  and  $\gamma_{x\theta}$  are

$$\begin{aligned} \varepsilon_{xx} &= \frac{\partial u_1}{\partial x} + \frac{1}{2} \left[ \left( \frac{\partial u_1}{\partial x} \right)^2 + \left( \frac{\partial u_2}{\partial x} \right)^2 + \left( \frac{\partial u_3}{\partial x} \right)^2 \right] \\ \varepsilon_{\theta\theta} &= \frac{1}{\rho_r} \left( \frac{\partial u_2}{\partial \theta} + u_3 \right) + \frac{1}{2\rho_r^2} \left[ \left( \frac{\partial u_1}{\partial \theta} \right)^2 + \left( \frac{\partial u_3}{\partial \theta} - u_2 \right)^2 + \left( \frac{\partial u_2}{\partial \theta} + u_3 \right)^2 \right] \\ \gamma_{x\theta} &= \left( \frac{\partial u_1}{\rho_r \partial \theta} + \frac{\partial u_2}{\partial x} \right) + \frac{1}{\rho_r} \left[ \left( \frac{\partial u_1}{\partial x} \frac{\partial u_1}{\partial \theta} \right) + \frac{\partial u_2}{\partial x} \left( \frac{\partial u_2}{\partial \theta} + u_3 \right) + \frac{\partial u_3}{\partial x} \left( \frac{\partial u_3}{\partial \theta} - u_2 \right) \right] \end{aligned} \tag{2.2}$$

where  $\rho_r = R + z$ . Substituting Eqs. (2.2) into Eqs. (2.1), the strain components are rewritten and abbreviated as

$$\varepsilon_{xx} = \varepsilon_{x,0} + zk_x \quad \varepsilon_{\theta\theta} = \varepsilon_{\theta,0} + zk_\theta \quad \gamma_{x\theta} = \gamma_{x\theta,0} + zk_{x\theta} \tag{2.3}$$

where  $\varepsilon_{x,0}$ ,  $\varepsilon_{\theta,0}$  and  $\gamma_{x\theta,0}$  are corresponding strain components of the middle surface, while  $k_x$ ,  $k_\theta$  and  $k_{x\theta}$  are changes of curvature and torsion of the middle surface. The shell theories distinguish from each other by the expression  $\Theta_1$  and  $\Theta_2$  in Eqs. (2.1) based on different deformation assumptions. In Donnell's shell theory,  $\Theta_1 = \partial w / \partial x$ ,  $\Theta_2 = \partial w / R \partial \theta$ , and the variations of the middle surface in Eqs. (2.3) are

$$\begin{aligned} \varepsilon_{x,0} &= \frac{\partial u}{\partial x} + \frac{1}{2} \left( \frac{\partial w}{\partial x} \right)^2 & \varepsilon_{\theta,0} &= \frac{\partial v}{R \partial \theta} + \frac{w}{R} + \frac{1}{2} \left( \frac{\partial w}{R \partial \theta} \right)^2 \\ \gamma_{x\theta,0} &= \frac{\partial u}{R \partial \theta} + \frac{\partial v}{\partial x} + \frac{\partial w}{\partial x} \frac{\partial w}{R \partial \theta} \end{aligned} \tag{2.4}$$

and

$$k_x = -\frac{\partial^2 w}{\partial x^2} \quad k_\theta = -\frac{\partial^2 w}{R^2 \partial \theta^2} \quad k_{x\theta} = -2\frac{\partial^2 w}{R \partial x \partial \theta} \quad (2.5)$$

In the cylindrical coordinate system, the equations of motion with respect to the original configuration are (Kumar *et al.*, 2015)

$$\begin{aligned} \frac{\partial T_{xx}}{\partial x} + \frac{\partial T_{\theta x}}{\rho_r \partial \theta} + \frac{\partial T_{zx}}{\partial z} + \frac{T_{zx}}{\rho_r} + X &= 0 \\ \frac{\partial T_{x\theta}}{\partial x} + \frac{\partial T_{\theta\theta}}{\rho_r \partial \theta} + \frac{\partial T_{z\theta}}{\partial z} + \frac{T_{z\theta} + T_{\theta z}}{\rho_r} + Y &= 0 \\ \frac{\partial T_{xz}}{\partial x} + \frac{\partial T_{\theta z}}{\rho_r \partial \theta} + \frac{\partial T_{zz}}{\partial z} + \frac{T_{zz} - T_{\theta\theta}}{\rho_r} + Z &= 0 \end{aligned} \quad (2.6)$$

where  $X$ ,  $Y$  and  $Z$  are the sum of the body force and inertia force along  $x, \theta, z$  directions, respectively.  $T_{ij}$  ( $i, j = x, \theta, z$ ) are the components of the first Piola-Kirchhoff (1st P-K) stress tensor, which can be expressed in terms of the symmetric second Piola-Kirchhoff (2nd P-K) stresses  $\sigma_{ij}$  by the relation

$$T_{ij} = \sum_{k=1}^3 \sigma_{ik} \frac{\partial a_j}{\partial x_k} \quad (2.7)$$

where  $x_1 = x$ ,  $x_2 = R\theta$  and  $x_3 = z$ .  $a_i = x_i + u_i$ , ( $i = 1, 2, 3$ ) is the coordinate of a generic point inside the deformed shell. Here, ( $i = 1, 2, 3$ ) corresponds to the direction  $(x, \theta, z)$ , respectively. With the help of Eq. (2.7), the equations of motion can be expressed in terms of the 2nd P-K stress. Then, integrating the new equations of motion through thickness of the shell leads to the force equilibrium equations as

$$\begin{aligned} \frac{\partial N_x}{\partial x} + \frac{\partial N_{x\theta}}{R \partial \theta} - ch \frac{\partial u(x, \theta, t)}{\partial t} - \rho h \frac{\partial^2 u(x, \theta, t)}{\partial t^2} &= 0 \\ \frac{\partial N_\theta}{R \partial \theta} + \frac{\partial N_{x\theta}}{\partial x} + \frac{Q_\theta}{R} - ch \frac{\partial v(x, \theta, t)}{\partial t} - \rho h \frac{\partial^2 v(x, \theta, t)}{\partial t^2} &= 0 \\ \frac{\partial Q_x}{\partial x} + \frac{\partial Q_\theta}{R \partial \theta} + N_x \frac{\partial^2 w(x, \theta, t)}{\partial x^2} + N_{x\theta} \frac{\partial^2 w(x, \theta, t)}{R \partial x \partial \theta} + N_{\theta x} \frac{\partial^2 w(x, \theta, t)}{R \partial x \partial \theta} \\ + N_\theta \frac{\partial^2 w(x, \theta, t)}{R^2 \partial \theta^2} - \frac{N_\theta}{R} + \left( \frac{\partial N_x}{\partial x} + \frac{\partial N_{\theta x}}{R \partial \theta} \right) \frac{\partial w(x, \theta, t)}{\partial x} \\ + \left( \frac{\partial N_{x\theta}}{\partial x} + \frac{\partial N_\theta}{R \partial \theta} \right) \frac{\partial w(x, \theta, t)}{R \partial \theta} - ch \frac{\partial w(x, \theta, t)}{\partial t} - \rho h \frac{\partial^2 w(x, \theta, t)}{\partial t^2} + P &= 0 \end{aligned} \quad (2.8)$$

Multiplying the first two equations of motion by  $z$  and integrating them through thickness, the moment equilibrium equations are obtained

$$\frac{\partial M_x}{\partial x} + \frac{\partial M_{\theta x}}{R \partial \theta} - Q_x = 0 \quad \frac{\partial M_{x\theta}}{\partial x} + \frac{\partial M_\theta}{R \partial \theta} - Q_\theta = 0 \quad (2.9)$$

where

$$N_x = \int_{-h/2}^{h/2} \sigma_{xx} \left( 1 + \frac{z}{R} \right) dz \quad N_\theta = \int_{-h/2}^{h/2} \sigma_{\theta\theta} dz$$

$$\begin{aligned}
 N_{x\theta} &= \int_{-h/2}^{h/2} \sigma_{x\theta} \left(1 + \frac{z}{R}\right) dz & N_{\theta x} &= \int_{-h/2}^{h/2} \sigma_{\theta x} dz \\
 Q_x &= \int_{-h/2}^{h/2} \sigma_{xz} \left(1 + \frac{z}{R}\right) dz & Q_\theta &= \int_{-h/2}^{h/2} \sigma_{\theta z} dz \\
 M_x &= \int_{-h/2}^{h/2} \sigma_{xx} \left(1 + \frac{z}{R}\right) z dz & M_\theta &= \int_{-h/2}^{h/2} \sigma_{\theta\theta} z dz \\
 M_{x\theta} &= \int_{-h/2}^{h/2} \sigma_{x\theta} \left(1 + \frac{z}{R}\right) z dz & M_{\theta x} &= \int_{-h/2}^{h/2} \sigma_{\theta x} z dz
 \end{aligned} \tag{2.10}$$

where  $\rho$  is the material density, and  $c$  is the equivalently viscous damping coefficient of the material.  $P$  can be regarded as the external loading along the radial direction. External loadings in other directions are not considered.

In addition, the constitutive relation for linearly elastic plane stress problems is

$$\sigma_{xx} = \frac{E}{1 - \mu^2} (\varepsilon_{xx} + \mu \varepsilon_{\theta\theta}) \quad \sigma_{\theta\theta} = \frac{E}{1 - \mu^2} (\varepsilon_{\theta\theta} + \mu \varepsilon_{xx}) \quad \sigma_{x\theta} = \frac{E}{2(1 + \mu)} \gamma_{x\theta} \tag{2.11}$$

where  $E$  is Young's modulus of the material, and  $\mu$  is Poisson's ratio.

### 3. Governing equations for infinitely long cylindrical shells

For infinitely long shells, changes of the quantities along the axial direction as well as the axial displacement are regarded as zero. Additionally, viscous damping of the material is ignored. Therefore, Eqs. (2.8)<sub>1</sub> and (2.9)<sub>1</sub> are naturally satisfied based on these two assumptions, whereas Eqs. (2.8)<sub>2</sub> and (2.8)<sub>3</sub> are reduced to

$$\begin{aligned}
 \frac{\partial N_\theta}{R \partial \theta} + \frac{1}{R} \frac{\partial M_\theta}{R \partial \theta} - \rho h \frac{\partial^2 v(x, \theta, t)}{\partial t^2} &= 0 \\
 \frac{\partial^2 M_\theta}{R^2 \partial \theta^2} - N_\theta \left( \frac{1}{R} + k_\theta \right) + \frac{\partial N_\theta}{R \partial \theta} \frac{\partial w(x, \theta, t)}{R \partial \theta} - \rho h \frac{\partial^2 w(x, \theta, t)}{\partial t^2} + P &= 0
 \end{aligned} \tag{3.1}$$

Substituting Eqs. (2.3) and (2.11) into Eq. (2.10) gives the expressions of  $N_\theta$  and  $M_\theta$  as

$$N_\theta = \frac{Eh}{1 - \mu^2} \varepsilon_{\theta,0} \quad M_\theta = \frac{Eh^3}{12(1 - \mu^2)} k_\theta \tag{3.2}$$

The middle surface strain  $\varepsilon_{\theta,0}$  and curvature change  $k_\theta$  based on Donnell's theory are given in Eqs. (2.4) and (2.5).

However, it is known that Donnell's shell theory breaks down for non-shallow, long cylindrical shells experiencing large deformations, which is revealed in the expression of curvature change (Xue *et al.*, 2013). According to Donnell's theory, though some predominant nonlinear terms are retained, the curvature changes are expressed by linear functions of  $w$ . For radial displacements exceeding thickness of the shell, the change of curvature due to radius reduction can be obvious and should be comprised of two parts. Firstly, the change of curvature could be caused by shell radius variation, and can be rewritten as

$$k'_\theta = \frac{1}{R + w} - \frac{1}{R} = -\frac{w}{R(R + w)} \tag{3.3}$$

Secondly, bending deformation of the shell wall also contributes to the change of curvature. Considering curvatures of the middle surface resulted from bending in the deformed and undeformed configurations, and rewriting the expressions of the curvature in terms of the radial displacement and its derivatives, leads to the change of curvature as

$$k''_{\theta} = \frac{-\partial^2 w}{R^2 \partial \theta^2} \left[ 1 + \left( \frac{\partial w}{R \partial \theta} \right)^2 \right]^{-3/2} \quad (3.4)$$

Therefore, for the buckling problem in this paper, the change of curvature  $k_{\theta}$  defined in Eq. (2.5) can be replaced by

$$\tilde{k}_{\theta} = k'_{\theta} + k''_{\theta} = -\frac{w}{R(R+w)} - \frac{\partial^2 w}{R^2 \partial \theta^2} \left[ 1 + \left( \frac{\partial w}{R \partial \theta} \right)^2 \right]^{-3/2} \quad (3.5)$$

By substituting the change of curvature in Eq. (3.5) and the middle surface strain  $\varepsilon_{\theta,0}$  in Eq. (2.4) into Eqs. (3.1) and (3.2), the governing equations can be obtained in terms of middle surface displacements. The ultimate expressions are omitted here for conciseness. These equations can degenerate into those used in (Lindberg and Florence, 1987) by omitting the term  $(\partial w / R \partial \theta)^2$ . And the reduced equation of motion in the circumferential direction is

$$\frac{\partial^2 M_{\theta}}{R^2 \partial \theta^2} - N_{\theta} \left( \frac{1}{R} + k_{\theta L} \right) - \rho h \frac{\partial^2 w(x, \theta, t)}{\partial t^2} + P = 0 \quad (3.6)$$

where  $N_{\theta}$  and  $M_{\theta}$  are defined in Eqs. (3.2).  $\varepsilon_{\theta,0}$  in Eq. (3.2)<sub>1</sub> is rewritten as  $w/R$  and  $k_{\theta}$  in Eq. (3.1)<sub>2</sub> is replaced by  $k_{\theta L} = w/R^2 - \partial^2 w / R^2 \partial \theta^2$ .

Moreover, in order to quantitatively describe the buckling degree of cylindrical shells at a certain time during the buckling procedure, a new parameter is defined as

$$c_0 = \frac{1}{\pi r_0^2} \int_0^{2\pi} |r_0^2 - r_1^2| d\theta \quad (3.7)$$

which means the ratio of area surrounded by the buckled shell shape and the corresponding deformed circular line without buckling to the circular area.  $r_1$  in Eq. (3.7) denotes radius of the buckled cylindrical shell,  $r_0$  is the corresponding radius without the occurrence of buckling.

## 4. Solution procedure and validation

### 4.1. Solution procedure

The finite difference method (FDM) is employed to solve the partial differential equations. The scheme of central difference is applied to deal with the derivatives of displacements with respect to coordinates as

$$\begin{aligned} \left( \frac{\partial f}{\partial \theta} \right)_m &= \frac{f_{m+1} - f_{m-1}}{2\Delta\theta} & \left( \frac{\partial^2 f}{\partial \theta^2} \right)_m &= \frac{f_{m+1} - 2f_m + f_{m-1}}{(\Delta\theta)^2} \\ \left( \frac{\partial^3 f}{\partial \theta^3} \right)_m &= \frac{(f_{m+2} - f_{m-2}) - 2(f_{m+1} - f_{m-1})}{2(\Delta\theta)^3} \\ \left( \frac{\partial^4 f}{\partial \theta^4} \right)_m &= \frac{(f_{m+2} - f_{m-2}) - 4(f_{m+1} + f_{m-1}) + 6f_m}{(\Delta\theta)^4} \end{aligned} \quad (4.1)$$

where  $f$  refers to displacement variations,  $\Delta\theta$  is the grid size, and  $m$  is the number of an element. As for the partial derivative with respect to time, the following forward difference method is used

$$\left( \frac{\partial^2 f}{\partial t^2} \right)^n = \frac{1}{\Delta t} \left[ \left( \frac{\partial f}{\partial t} \right)^{n+1} - \left( \frac{\partial f}{\partial t} \right)^n \right] \quad (4.2)$$

where  $\Delta t$  is the time step, and  $n$  is the step number. The displacement can be obtained by integrating Eq. (4.2) as

$$f^{n+1} = f^n + \Delta t \left( \frac{\partial f}{\partial t} \right)^{n+1} \tag{4.3}$$

Besides, the condition of periodicity of the cylindrical shell needs to be considered, namely

$$f(\theta) = f(\theta + 2\pi) \tag{4.4}$$

#### 4.2. Validation

In order to validate the presented shell-buckling model, a cylindrical shell with  $R = 48.5$  mm and  $h = 1.5$  mm is taken as an example. The shell is subjected to a particularly non-uniform impact pressure on the opposite side to the shell outer surface. This pressure easily causes a relatively large radial displacement and strain and makes the effects of the added nonlinear terms in the presented model significant. The initial displacement and velocity of the shell are zero. The shell is made of steel. Without loss of generality, the shell is assumed to deform elastically. The impact pressure profile is illustrated in Fig. 2, and can be mathematically expressed as

$$P(\theta, t) = \begin{cases} P_0 e^{-7t/t_0} \sin(4\theta) & \theta \in \left[0, \frac{\pi}{4}\right] \wedge \left[\pi, \frac{5\pi}{4}\right] \\ 0 & \text{otherwise} \end{cases} \tag{4.5}$$

in which  $P_0$  is the loading magnitude and  $t_0$  represents the total calculation time. The range  $[0, \pi/4] \wedge [\pi, 5\pi/4]$  can be regarded as the loaded region of the shell.  $P_0 = 400$  MPa and  $t_0 = 100$   $\mu$ s are adopted in this paper for numerical calculations.

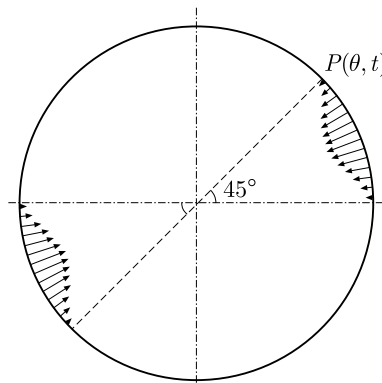


Fig. 2. Pressure profile applied on the cylindrical shell

To show the accuracy and efficiency of the presented model, the radial displacements distributed along the circumferential direction at the instant of  $t = 100$   $\mu$ s are displayed in Fig. 3. It should be mentioned that the results from the FE model without particular assumptions on the deformation mechanism are thought to be more accurate, whereas the assumptions are made in both analytical models. The red curve is calculated by a commercial FEM software in a three-dimensional configuration. The FEM model is processed by Abaqus/Explicit with 4-node doubly curved general-purpose shell elements. 72000 elements are used in total. This model adopts assumption (H2) in this work, but the effect of large deformation to the equilibrium position of the structure is considered in the FEM model. The other two curves are calculated by the model presented in this paper and the model by Lindberg and Florence (1987), respectively. It is clear that the results of the presented model agrees well with those of FEM, while the model by Lindberg and Florence (1987), shown by the blue dash line, deviates from FEM apparently.

Both the FEM and current models give an inward movement of middle points in the loaded regions, while the movement of the middle points predicted by Lindberg and Florence (1987) is outward. Thus, the presented model is more credible than that by Lindberg and Florence (1987). Therefore, the presented model is able to deal with transient impact problems of thin-walled cylindrical shells undergoing large displacements.

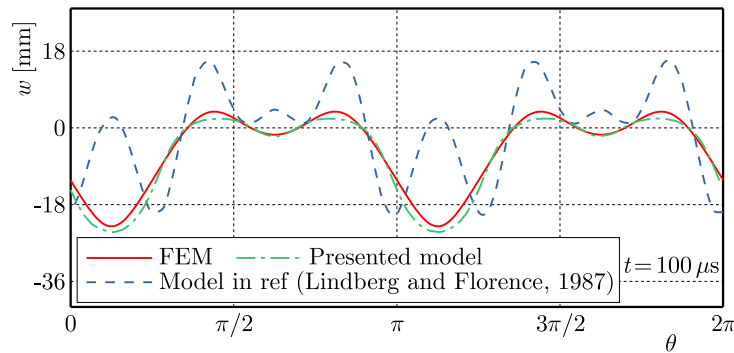


Fig. 3. Radial displacements at  $100 \mu\text{s}$  of different models

## 5. Shell buckling under randomly radial impact pressures

In this Section, the dynamic buckling behavior of the thin-walled cylindrical shell under radial impact pressures randomly distributed in the circumferential direction is investigated. Explosive devices, like shaped-charge weapons and oil well perforators, are usually subjected to impact pressures that have significantly radial components over 100 MPa, and metal shells always deform plastically. Thus, a constitutive equation of plasticity should be used instead of the elastic model in Eqs. (2.11). The widely used Johnson-Cook constitutive model without the temperature effect is chosen in the following analysis and expressed as

$$\sigma = (A + B\varepsilon^n) \left( 1 + C \ln \frac{\dot{\varepsilon}}{\dot{\varepsilon}_0} \right) \quad (5.1)$$

where the reference strain rate  $\dot{\varepsilon}_0$  is taken as  $1.0 \text{ s}^{-1}$ .  $A$ ,  $B$ ,  $n$  and  $C$  are coefficients depending on the material. For simplicity, the tangent modulus, defined as  $E_t = d\sigma/d\varepsilon$ , is adopted to replace Young's modulus in Eqs. (2.11) and updated in every numerical time step to simulate the plastic behavior using the constitutive equation.

Naturally, uniform impact pressures are prone to be influenced by randomly environmental factors leading to nonuniformity of the pressures. Suppose that the impact pressure distributes in the form of white noise as

$$P(\theta, t) = P'(t) \left[ 1 + \sum_{n=1}^N \gamma_n \cos(n\theta + \varphi_n) \right] \quad (5.2)$$

in which  $N$  is the term number of the Fourier series. The parameters  $\gamma_n$  and  $\varphi_n$  denote the disturbance magnitude and random phase angle, respectively. Subsequently, the effect of random characteristic, material property and structural size on the dynamic buckling behavior of the shell are investigated. The shell examples taken in the following analysis are listed in Table 1.

### 5.1. Effect of random characteristics of pressure

Three groups of pressure parameters are chosen to study the effect of random characteristics on the buckling behavior of the shell. Figure 4 shows radial pressure distributions at the initial

**Table 1.** Shell cases with different materials and sizes (Zhang *et al.*, 2015)

Case No.	1	2	3	4	5
Material	4043 Steel	7075-T6 Al	7075-T6 Al	7075-T6 Al	OFHC COPPER
$\rho$ [kg/m <sup>3</sup> ]	7830	2700	2700	2700	8960
$E$ [GPa]	200	86	86	86	124
$\mu$	0.29	0.3	0.3	0.3	0.34
$R$ [mm]	40	40	40	40	40
$h$ [mm]	1.5	1.5	2	2.5	1.5
$A$ [MPa]	792	473	473	473	90
$B$ [MPa]	510	210	210	210	292
$n$	0.26	0.38	0.38	0.38	0.31
$C$	0.014	0.033	0.033	0.033	0.025

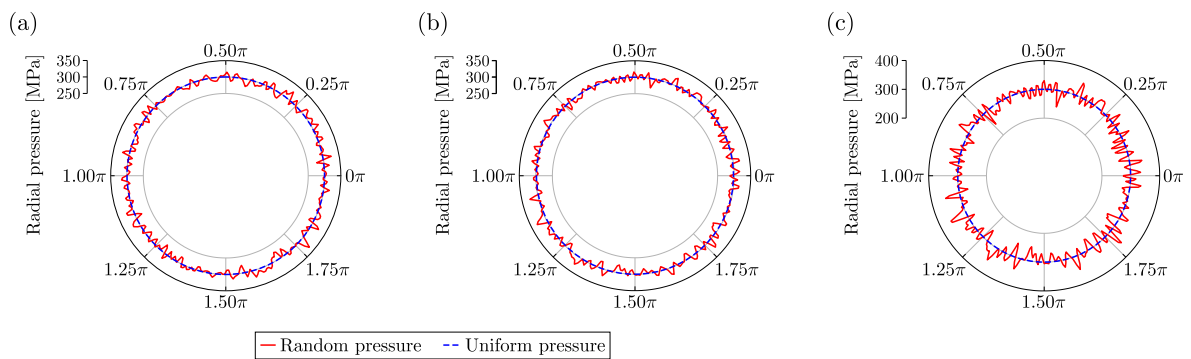


Fig. 4. Initial pressure distributions: (a)  $\gamma_n = 0.005$ , random phase I; (b)  $\gamma_n = 0.005$ , random phase II; (c)  $\gamma_n = 0.01$ , random phase II

time of three cases, in which  $P'(t) = 300$  MPa and  $N = 100$ . The solid red line and dash blue line represent the pressure with white noise along the circumferential direction and the uniform pressure, respectively.

The parameters  $\gamma_n$  and  $\varphi_n$  vary from one case to another. The pressures in Figs. 4a and 4b have the equal perturbation amplitude ( $\gamma_n = 0.005$ ) but different phase angles. The perturbation amplitude of the pressure in Fig. 4c is twice of that in Fig. 4b ( $\gamma_n = 0.01$ ), but sharing the equal phase angles. The pressures in Figs. 4a, 4b and 4c are simply called pressure (a), pressure (b) and pressure (c), hereafter.

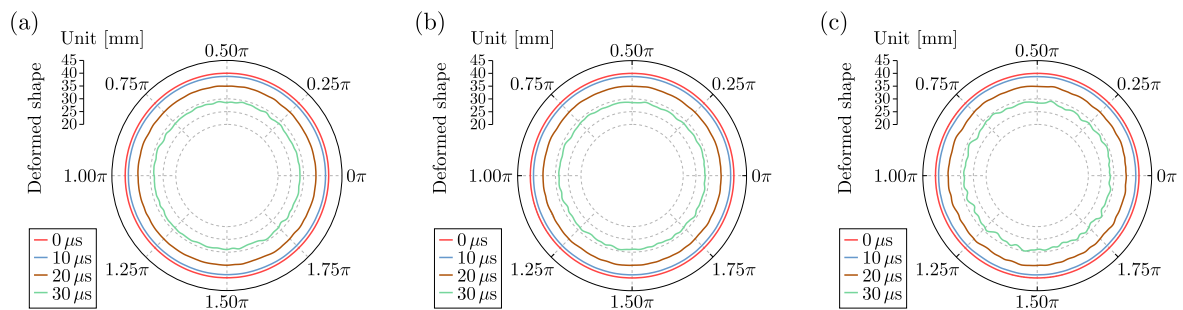


Fig. 5. Deformation evolution under: (a) pressure (a), (b) pressure (b), (c) pressure (c)

Under pressures shown in Fig. 4, deformation evolutions of cylindrical shell No. 1 in Table 1 are exhibited in Fig. 5. Taking Fig. 5a for instance, the wrinkled circles from the outside to inside represent the deformed shape of the cylindrical shell at different times. It is clear that the buckling degree is gradually magnified in a certain deformation profile with an increase of time,

which is visualized in Figs. 5b and 5c as well. In addition, the mean deformation values over the circumferential direction at an instant of  $30\ \mu\text{s}$  are almost the same for the three figures. The shell under pressures (a) and (b) shows the similar buckling degree, while the buckling in Fig. 5c is much severer than the former two. It is worth mentioning that a continuous circle deformation without buckling can be depicted for a uniform pressure  $P = P'(t)$ , which is omitted here for conciseness.

In order to show the buckling degree of the cylindrical shell under different pressures more clearly, Fig. 6 draws the evolution of  $c_0$  defined in Eq. (3.7). It is clear that  $c_0$  increases almost monotonously for the three non-uniform pressures, which means that the buckling degree is becoming stronger as the shell collapses. The values of  $c_0$  for pressures (a) and (b) show almost no discrepancy, while  $c_0$  for pressure (c) is much higher. This is consistent with the pressure characteristics, and the effectiveness of  $c_0$  to describe the buckling degree quantitatively is justified. Furthermore, Fig. 6 tells us that the threshold value of  $c_0$  can be used as the tolerance limit of shell buckling under non-uniform pressures.

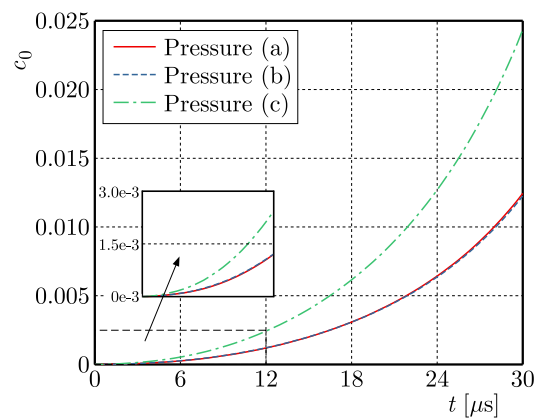


Fig. 6.  $c_0$  versus time for different pressures

The crest number of the deformed cylindrical shell is sometimes concerned in the engineering. According to Fig. 5, the crest number calculated for the three pressures is around 26. And further analyses indicate that this number is dependent on the material property and the value of  $N$  in Eq. (5.2).

In summary, the magnitude of uniform pressure  $P'$  can remarkably influence the mean deformation value of the cylindrical shell, and the disturbance magnitude  $\gamma_n$  is responsible for the buckling degree. The random phase angle  $\varphi_n$  affects the distribution of pressure, thus it is responsible for the exact deformation contour of the cylindrical shell. The loading itself as well as perturbation do not always change for a particular engineering application. Hence, designing a suitable structure and choosing a proper material are the conventional measures to avoid buckling. This will be discussed in detail in the following sections.

## 5.2. Effect of material

In order to study the effect of materials on the dynamic buckling behavior, No. 1, 2 and 5 shells in Table 1 made of steel, aluminum and copper with the same size are taken into consideration. The loading parameters are set to be  $P'(t) = 300\ \text{MPa}$ ,  $N = 100$ , and  $\gamma_n = 0.005$ . The random phase angles are the same as those in Fig. 4b.

Figure 7a illustrates the radius of the cylindrical shell at  $t = 20\ \mu\text{s}$ , and Fig. 7b shows the evolution of  $c_0$  over time. Under the same pressure condition, the radial displacement as well as the radius perturbation magnitude of the aluminum shell is larger than those of steel and copper shells. Among the three materials, the aluminum shell experiences the most violent

buckling deformation, which is revealed by the value of  $c_0$  in Fig. 7b. At the time  $t = 20 \mu\text{s}$ ,  $c_0$  of the aluminum shell is almost 10 times of that of steel and copper shells. The mean radius of the steel shell (35.0 mm) and copper shell (35.6 mm) are close to each other at  $t = 20 \mu\text{s}$ . Besides, the buckling degrees of steel and copper shells show little difference. Such buckling of the aluminum shell in this case is sometimes catastrophic and cannot be accepted. Then, when the aluminum shell is used in such a situation, optimization of the size of the cylindrical shell might be needed.

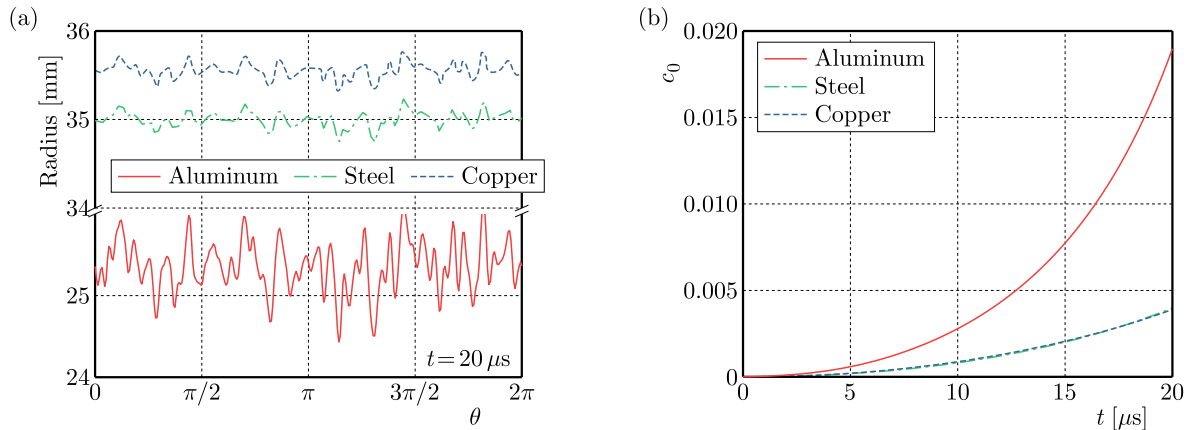


Fig. 7. (a) Radius of shells with different materials ( $t = 20 \mu\text{s}$ ), (b)  $c_0$  versus time for different shell materials

### 5.3. Effect of shell thickness

In this Section, the effects of the shell thickness  $h$  on the buckling of cylindrical shells are investigated. The pressure is retained the same as that in Section 5.2. Shells No. 2-4 in Table 1 are taken for calculation in this Section.

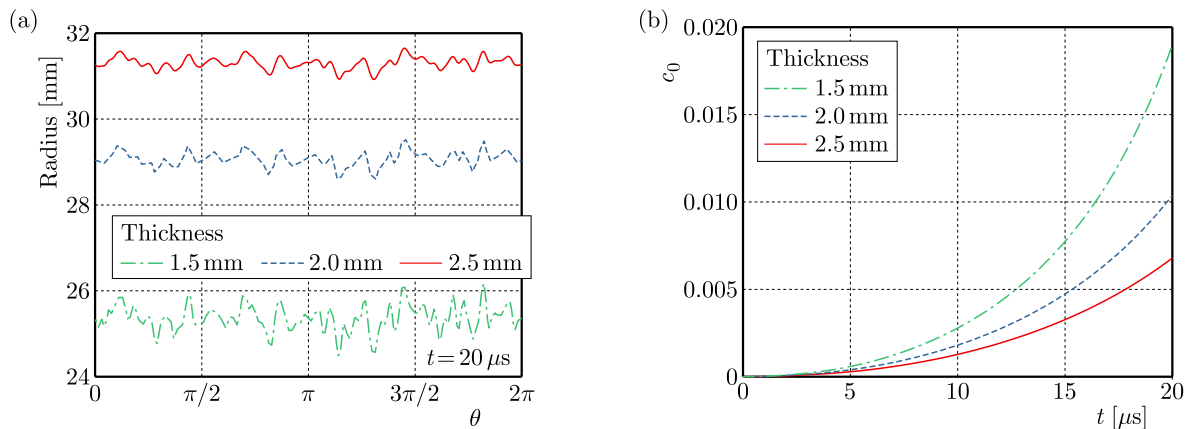


Fig. 8. (a) Radius of shells with different thickness, (b)  $c_0$  versus time for shells with different thickness

Figure 8a shows results for the radius of aluminum shells with different  $h$ . At the instant of  $t = 20 \mu\text{s}$ , the mean radial displacement increases with the reduction of  $h$ , leading to an decrease in the radius. Meanwhile, the perturbation magnitude is relatively larger for a thinner cylindrical shell. The buckling degree parameter  $c_0$ , as expected, increases during the deformation process regardless of the wall thickness, as revealed in Fig. 8b. And the value of  $c_0$  is higher when the shell is thinner. The crest numbers of the three shells are 31, 23 and 18 for the wall thickness of 1.5 mm, 2 mm and 2.5 mm, respectively. The effect of thickness on the crest number has also been confirmed by Lindberg and Florence (1987).

## 6. Conclusion

By considering the nonlinear terms in the geometrical equation of the cylindrical shell and maintaining the curvature variation due to a significant change of the shell radius, a buckling model is proposed to study large deformation behavior of the shell under radial impact pressures randomly distributing in the circumferential direction. Green's strain tensor and the 1st P-K stress tensor are employed to describe the large deformation, and a new parameter is introduced to quantitatively judge the buckling degree of the shell. The following conclusions can be drawn from the numerical analyses:

- The buckling model proposed in this paper can accurately describe the large deformation behavior of the shell under non-uniform pressures.
- The buckling shape of the shell after deformation is contributed by the magnitude of the uniform pressure, the magnitude of disturbance and the angle phase of random disturbance. A more uniform pressure distribution produces a more circular shape after deformation.
- The buckling behavior of the shell is dependent on the material properties remarkably. Aluminum shells buckle more easily compared with steel and copper ones under the same pressure condition.
- The buckling degree can be effectively described by the defined parameter  $c_0$  which increases with reduction of the shell wall thickness.

### *Acknowledgements*

This work was partially supported by the National Natural Science Foundation of China (Grant Nos. U2141246 and 11702137).

## References

1. AMABILI M., 2008, *Nonlinear Vibrations and Stability of Shells and Plates*, Cambridge University Press, New York
2. AMABILI M., PAÏDOUSSIS M.P., 2003, Review of studies on geometrically nonlinear vibrations and dynamics of circular cylindrical shells and panels, with and without fluid-structure interaction, *Applied Mechanics Reviews*, **56**, 349-381
3. AN H., ZHOU L., WEI X., AN W., 2016, Nonlinear analysis of dynamic stability for the thin cylindrical shells of supercavitating vehicles, *Advances in Mechanical Engineering*, **9**, 1-15
4. BEN-HAIM Y., 1993, Convex models of uncertainty in radial pulse buckling of shells, *Transactions of the ASME. Journal of Applied Mechanics*, **60**, 683-688
5. BYKOV A.I., DOLOTENKO M.I., 2015, An MC-1 cascade magnetocumulative generator of multi-megagauss magnetic fields – ideas and their realization, *Instruments and Experimental Techniques*, **58**, 531-538
6. DARABI M., GANESAN R., 2016, Non-linear dynamic instability analysis of laminated composite cylindrical shells subjected to periodic axial loads, *Composite Structures*, **147**, 168-184
7. ELISHAKOFF I., 2000, Uncertain buckling: Its past, present and future, *International Journal of Solids and Structures*, **37**, 6869-6889
8. FARID J., 2012, *Importance of Perforation Process and its Techniques*, Dalhousie University, Nova Scotia
9. GU W., TANG W., LIU T., 1996, Dynamic pulse buckling of cylindrical shells subjected to external impulsive loading, *Journal of Pressure Vessel Technology*, **118**, 33-37
10. HUTCHINSON J., 1965, Axial buckling of pressurized imperfect cylindrical shells, *AIAA Journal*, **3**, 1461-1466

11. HUTCHINSON J.W., 2016, Buckling of spherical shells revisited, *Proceedings of the Royal Society A-Mathematical Physical and Engineering Sciences*, **472**
12. JONES N., OKAWA D.M., 1976, Dynamic plastic buckling of rings and cylindrical shells, *Nuclear Engineering and Design*, **37**, 125-147
13. KARAGIOZOVA D., ALVES M., 2008, Dynamic elastic-plastic buckling of structural elements: A review, *Applied Mechanics Reviews*, **61**, 040803
14. KUMAR A., DAS S., WAHI P., 2011, Dynamic buckling of thin-walled cylindrical shells subjected to fluctuating radial loads, *21st International Conference on Structural Mechanics in Reactor Technology*
15. KUMAR A., LAL DAS S., WAHI P., 2015, Instabilities of thin circular cylindrical shells under radial loading, *International Journal of Mechanical Sciences*, **104**, 174-189
16. KUNDALWAL S.I., SHINGARE K.B., 2020, Electromechanical response of thin shell laminated with flexoelectric composite layer, *Thin-Walled Structures*, **157**, 107138
17. LINDBERG H.E., 1992a, An evaluation of convex modeling for multimode dynamic buckling, *Transactions of the ASME. Journal of Applied Mechanics*, **59**, 929-936
18. LINDBERG H.E., 1992b, Convex models for uncertain imperfection control in multimode dynamic buckling, *Transactions of the ASME. Journal of Applied Mechanics*, **59**, 937-945
19. LINDBERG H.E., FLORENCE A.L., 1987, *Dynamic Pulse Buckling Theory and Experiment*, Martinus Nijhoff Publishers, Dordrecht
20. SAHU S.K., DATTA P.K., 2007, Research advances in the dynamic stability behavior of plates and shells: 1987-2005-Part I: Conservative systems, *Applied Mechanics Reviews*, **60**, 65-75
21. SARAN S., AYISIT O., YAVUZ M.S., 2013, Experimental investigations on aluminum shaped charge liners, *Procedia Engineering*, **58**, 479-486
22. SURESH KUMAR R., KUNDALWAL S.I., RAY M.C., 2017, Control of large amplitude vibrations of doubly curved sandwich shells composed of fuzzy fiber reinforced composite facings, *Aerospace Science and Technology*, **70**, 10-28
23. TENG J.G., 1996, Buckling of thin shells: Recent advances and trends, *Applied Mechanics Reviews*, **49**, 263-274
24. WEI Z.G., BATRA R.C., 2006, Dynamic buckling of thin thermoviscoplastic cylindrical shell under radial impulsive loading, *Thin-Walled Structures*, **44**, 1109-1117
25. XU X., MA Y., LIM C.W., CHU H., 2006, Dynamic buckling of cylindrical shells subject to an axial impact in a symplectic system, *International Journal of Solids and Structures*, **43**, 3905-3919
26. XUE J., YUAN D., HAN F., LIU R., 2013, An extension of Karman-Donnell's theory for non-shallow, long cylindrical shells undergoing large deflection, *European Journal of Mechanics – A/Solids*, **37**, 329-335
27. ZHANG D., SHANGGUAN Q., XIE C., LIU F., 2015, A modified Johnson-Cook model of dynamic tensile behaviors for 7075-T6 aluminum alloy, *Journal of Alloys and Compounds*, **619**, 186-194